

Prediction of the Radiation Term in the Thermal Conductivity of Crosslinked Closed Cell Polyolefin Foams

O. A. ALMANZA,² M. A. RODRÍGUEZ-PÉREZ,¹ J. A. DE SAJA¹

¹ Departamento de Física de la Materia Condensada, Facultad de Ciencias, Universidad de Valladolid, 47011 Valladolid, Spain

² Departamento de Física, Universidad Nacional de Colombia, Santa Fé de Bogotá, D.C., Colombia

Received 26 April 1999; revised 12 November 1999; accepted 19 January 2000

ABSTRACT: The thermal conductivity and the cellular structure as well as the matrix polymer morphology of a collection of chemically crosslinked low-density closed cell polyolefin foams, manufactured by a high-pressure nitrogen gas solution process, have been studied. With the aid of a useful theoretical model, the relative contribution of each heat-transfer mechanism (conduction through the gas and solid phases and thermal radiation) has been evaluated. The thermal radiation can be calculated by using a theoretical model, which takes into account the dependence of this heat-transfer mechanism with cell size, foam thickness, chemical composition, and matrix polymer morphology. A simple equation, which can be used to predict the thermal conductivity of a given material, is presented. © 2000 John Wiley & Sons, Inc. *J Polym Sci B: Polym Phys* 38: 993–1004, 2000

Keywords: thermal conductivity; polyolefin foams; physical properties of foams; thermal radiation; cellular structure characterization

INTRODUCTION

It is well known that cellular materials, and in particular plastic foams, are widely used in thermal insulation in the low-ambient temperature range. Therefore, the knowledge of how the microscopic characteristics influence the thermal conductivity of these materials is an important subject that has been approached by different authors.^{1–9} Moreover, it is important to be able to predict the thermal conductivity of plastic foams by using theoretical models without adjustable parameters. These models would allow one to state conditions for minimizing the thermal conductivity and therefore, to reduce insulation costs and/or energy requirements.

The heat transfer through a foam is a consequence of four mechanisms: convection in the gas phase, conduction along the struts and cell walls of the solid polymer, conduction through the gas within the cells, and thermal radiation. Nowadays, the reduction of the thermal conductivity is mainly connected with minimizing the thermal radiation through the foam. Although, there are some equations,^{10–14} which can be used to estimate the heat transfer by radiation, it is difficult to check the validity of these models either because they included parameters that are very difficult to determine, or because of the complicated cellular structure of commercial plastic foams (which in many cases is nonhomogeneous and presents a high degree of anisotropy or/and residues of foaming agent in the cell walls, etc.). Therefore, these models cannot be strictly applied.

Polyolefin foams, manufactured by means of a high-pressure nitrogen gas solution process, are

Correspondence to: M. A. Rodríguez-Pérez (E-mail: marrod@wfsic.eis.uva.es)

Journal of Polymer Science: Part B: Polymer Physics, Vol. 38, 993–1004 (2000)
© 2000 John Wiley & Sons, Inc.

Table I. Main Characteristics of the Foams Under Study

Foams	ρ_f (kg/m ³)	L(cm)	k_{exp} (cm ⁻¹)	λ W/(m K)	θ_{carbon} (%)
LD15W	16.7	1.12	17.8	0.0374	
LD18W	22.5	0.96	5.8	0.0433	
LD24W	24.6	1.02	9.6	0.0372	
LD29W	30.7	1.11	13.9	0.0441	0
LD33W	32.0	1.10	15.0	0.0407	
LD33(1)W	32.5	1.08	18.6	0.0398	
LD50CNB	52.3	1.04	46.9	0.0413	12
LD60G	58.5	1.02	10.9	0.0475	0
LD70B	69.5	1.10	48.0	0.0456	4
HL34W	42.6	1.07	9.1	0.0486	
HL47W	44.2	1.04	8.3	0.0467	0
HL79B	71.3	1.06	29.1	0.0495	3
HL79W	74.0	0.78	7.8	0.0495	
HL79(2)W	81.0	0.99	8.2	0.0565n	
HL79(3)W	83.0	1.70	8.0	0.0592	
HD30W	23.5	1.07	9.3	0.0467	
MP24W	24.0	1.02	23.8	0.0359	
MP45B1	42.0	1.04	15.9	0.0423	0
VA25W	24.0	1.04	6.6	0.0424	
VA35W	34.2	1.07	14.3	0.0399	
VA65W	61.6	1.06	15.7	0.0459	
EV50O	45.3	1.12	11.5	0.0394	
EV50B	46.5	0.98	30.8	0.0370	3

W = White, O = Orange, B = Black, Bl = Blue, G = Green, ρ_f is the foam density, L is the thickness, k_{exp} is the extinction coefficient, λ is the thermal conductivity, and θ_{carbon} is the additional black carbon content in the polymeric matrix.

excellent materials for scientific studies because of some interesting features, such as:¹⁵

1. Lack of residues of solid foaming agent on the final foam
2. Almost isotropic cellular structure
3. Same cell shape for the different densities
4. Very similar physical characteristics of the solid polymer that comprises the cell walls and of the solid sheet from which the foam was made.

This morphology is appropriate to study the relationships between the microscopic structure and the physical properties and, in particular, these foams are adequate to check the validity of some of the theoretical models that have been proposed to predict the thermal conductivity of plastic foams.

Taking the previous notions in mind, an experimental study on the thermal conductivity of a collection of low-density polyolefin foams, made from a high-pressure nitrogen gas solution process, is presented in this work. The cellular struc-

ture and matrix polymer morphology of the foams are also analyzed in order to find out the main parameters of the different models.

MATERIALS

The product code, measured density (ρ_p), apparent color, thickness (L), extinction coefficient (k_{exp}) and thermal conductivity (λ) of the industrial materials under study are summarized in Table I. Six different types can be distinguished depending on the base polymer used to manufacture the foams. Some of the properties of those polymers are given in Table II. These properties were measured in the solid sheets that were used to manufacture the foams. The black foams presented a low content (between 2 and 3% in weight) of black carbon in their composition and the LD50CNB is an especial grade designed for applications where higher electrical conductivity is necessary. This material is a blend of LDPE and black carbon with a 10–12% content, in weight, of this last material.

Table II. Main Characteristics of the Solid Polymers Used To Manufacture the Foams

Polymer Description	ZFoams Code	ρ_0 (kg/m ³)	χ_c (%)	T_m (K)	λ (W/m K)
Low-Density Polyethylene (LDPE 100%)	LD	910	41.6	112.8	0.214
High-Density Polyethylene (HDPE 100%)	HD	950	66.2	130.8	0.1765
50% LDPE + 50% HDPE	HL	926	58.3	134.4	0.2246
Ethylene Vinyl Acetate Copolymer (EVA, 18% VA)	EV	928	23.3	82.2	0.2018
Ethylene Vinyl Acetate Copolymer (EVA, 9% VA)	VA	920	32.2	97.7	0.1224
Metallocene Polyethylene	MP	910	41.0	113.2	0.214

ρ_0 is the density, χ_c is the crystallinity, T_m is the melting point, and λ is the thermal conductivity.

These foamed samples are crosslinked closed cell polyolefin foams manufactured by a high-pressure nitrogen gas solution process, and have been kindly provided by Z-Foams Plc. (Croydon, U.K.). In this process, a polyolefin is compounded with a peroxide curing agent and extruded as a thick sheet, which is passed through a hot oven to effect crosslinking (gel content was approximately 40%). Slabs are cut from the extruded sheet and placed in an autoclave where they are subjected to high pressure (several hundred bars) of nitrogen gas at temperatures above the polymer softening point. Under these conditions, the nitrogen dissolves in the polymer. At the end of the solution stage, and after cooling, the pressure is reduced to zero gauge. The slabs, now containing nitrogen gas for expansion, are then placed under low pressure in a second autoclave and again heated above the polymer melting point. Release of the pressure then results in full expansion. By altering the saturation gas pressure, the amount of gas dissolved in the polymer and thus, the final foam density, is varied. Cell size can also be controlled by changing some industrial process parameters as for example the rate at which the pressure is reduced at the end of the solution stage or the gel content (a higher gel content results in materials with a lower cell size).

EXPERIMENTAL

Scanning Electron Microscopy (SEM)

Quantitative image analysis was used to assess the type of cellular structure, the mean cell size, the mean cell wall thickness, the anisotropy, as well as the relative fraction of polymer in the struts. For this purpose, cross sections of the

foams were microtomed at low temperature to provide a smooth surface which, after vacuum coating with gold, were examined by SEM using a JEOL JSM 820 microscope.

Each micrograph was analyzed by obtaining data from 10 horizontal reference lines. Apparent mean cell size (Φ) was estimated by calculating the number of cells that intersected each reference line and by dividing the appropriate reference length by the number of cells.¹⁶ About 400 cells were analyzed for each foam, this quantity was enough to obtain a representative population of the cellular structure.

To take into account the relationship between the average measured length of the randomly truncated cells and the real diameter of the cell, the previous result was multiplied by 1.62.¹⁷ A total of three micrographs were taken randomly over each specimen and subjected to cell size analysis. The standard deviation of these measurements was approximately $\pm 4\%$ of the average value.

The thickness of thirty cell walls, which were randomly chosen along the foam, was measured directly in the screen of the microscope. The average value of the thirty previous thicknesses was considered as the mean cell wall thickness (ξ) of the foam. The standard deviation of these measurements was approximately $\pm 6\%$ of the average value.

Finally, the fraction of mass in the struts (f_s) was obtained by means of the method proposed by Kuhn,⁵ measuring through four micrographs taken randomly over each specimen. The standard deviation was $\pm 6\%$ of the average value.

Differential Scanning Calorimetry (DSC)

Characteristic thermal properties were studied by means of a Mettler DSC30 differential scan-

ning calorimeter, previously calibrated with indium. The weights of the samples were approximately 2.5 mg. The experiments were performed between $-40\text{ }^{\circ}\text{C}$ and $200\text{ }^{\circ}\text{C}$ at $10\text{ }^{\circ}\text{C}/\text{min}$. Crystallinity (χ_c) was calculated from the DSC curve by dividing the measured heat of fusion by the heat of fusion of a 100% crystalline material (288 J/g for low-density polyethylene).¹⁸

Extinction Coefficient

The extinction coefficient was determined by applying Beer's law to measurements of transmissivity at different values of sample thickness. Transmissivity measurements were carried out over the infrared region (between 400 cm^{-1} and 4000 cm^{-1}), which is a range in which substantial radiant energy is emitted. Five thin slices of different thickness (between 0.5 and 3 mm) were cut for each material. The transmissivity measurements were performed in a Bomem FTIR spectrometer.

Density

Density measurements were carried out on the basis of Archimedes' principle, using the density determination kit designed for the AT261 Mettler balance.

Thermal Conductivity

A rapid K heat flow meter from Holometrix was used for the thermal measurements. The main characteristics of this equipment has been explained previously.¹⁹

Heat flow through the test sample (q) results from having a temperature gradient (δT) across the material. The thermal conductivity λ is defined according to Fourier's equation:

$$q = \lambda A \frac{\delta T}{L} \quad (1)$$

where A is the cross-sectional area of the sample and L , the sample thickness.

The measurements were made under steady heat flow conditions through the test sample in accordance with ASTM C518 and ISODIS 8301 methods. Square samples of 30 cm side and 11 mm thick approximately were used for all the experiments (except when the effect of the foam thickness was studied). A dispersion less than 1%

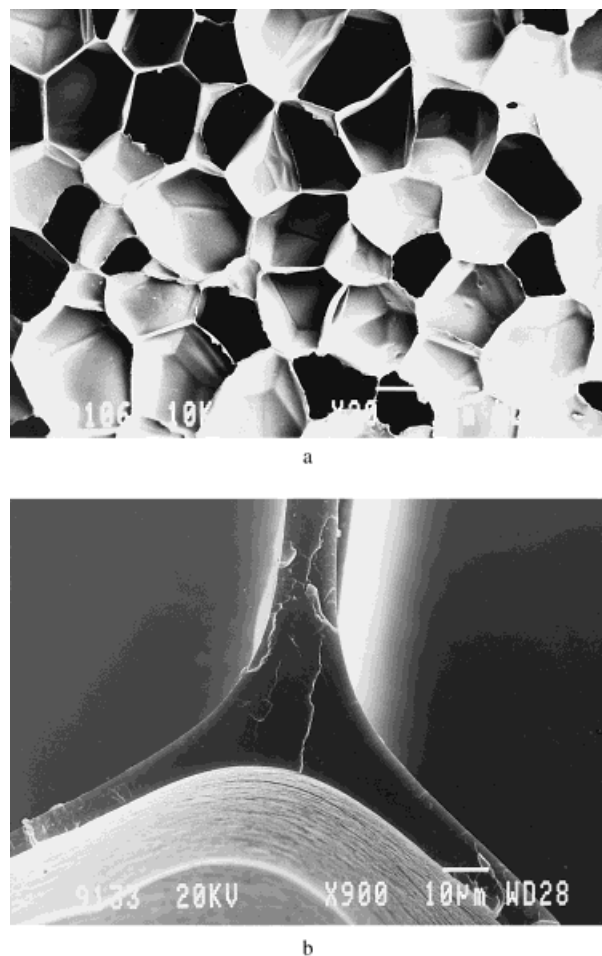


Figure 1. (a) Typical micrograph (LD50CNB) of the cellular structure of the foams under study; (b) typical micrograph (LD60G) of the cell walls and of one strut.

in two consecutive readings was taken as a criterion to ensure that the measurements were made under steady state conditions. The time lapse between readings was 20 min. The standard deviation of the measurements was approximately 5%.

EXPERIMENTAL RESULTS

Scanning Electron Microscopy (SEM)

Two representative images of the cellular structure of the samples under study are shown in Figure 1. A general view of the section of a cellular structure is presented in Figure 1(a). We first remark that the closed cell structure of these foams is isotropic and that no residues of foaming agent can be perceived. Moreover, in Figure 1(b) it is possible to examine a micrograph of charac-

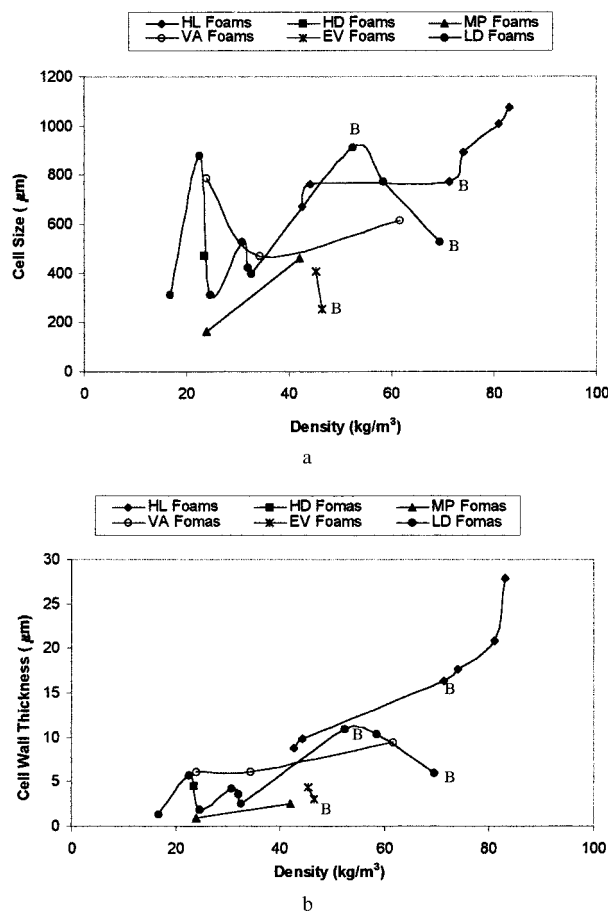


Figure 2. (a) Mean cell size as a function of the foam density for all the foams under study. B = Black foams. (b) Mean cell wall thickness as a function of the foam density for all the foams under study.

teristic cell walls (intersection of two cells) and of one strut (intersection of three or more cells).

The numerical values of the mean cell size and mean cell wall thickness as a function of the foam density have been presented in Figure 2(a,b) and in Table III. On the one hand, it can be stated that there is not a clear trend as a function of the density, which is due to the different process parameters utilized to manufacture different foams. On the other hand, it is evident that both properties present a similar dependence on density, which suggests there is a linear relationship between them. The data for the fraction of solid in the struts (f_s) are also given in Table III. This fraction was not negligible for these materials, which is characteristic of a cellular structure made from cell walls with a nonuniform thickness.

It is well known that for a given cell shape, it is possible to determine the mean cell wall thickness (ξ) by using the following equation:⁶

$$\Phi(1 - f_s) \frac{\rho_f}{\rho_0} = C\xi \quad (2)$$

where Φ is the mean cell size, (ρ_f) is the foam density, (ρ_0) is polymer base density and C is a constant that depends on the cell shape, and that, for instance, takes a value of 3.46 for pentagonal dodecahedrons⁶ and a value of 3.35 for tetrakaid-eahedral cells.²⁰

The experimental data for the LD, HD, MP, EV, and VA foams fits well the previous equation with a C value of 3.53 ± 0.40 (Fig. 3), which suggests that these foams have cells with comparable shapes, which in average, are similar to pentagonal dodecahedrons or tetrakaid-eahedrons. However, the previous fit gives a different C value for the HL foams, which in average, seems to have a different cell shape.

Differential Scanning Calorimetry (DSC)

The values of the crystallinity and melting point for each material are summarized in Table III.

From these data it can be deduced that the solid polymer that comprises the cell walls of foams of the same type has similar characteristics (same melting point and crystallinity). Moreover, the crystallinity of the solid from which the foam was manufactured is almost equal to that of the foams (Table II).

The results for the crystallinity and melting point of the six different types of foams under study are those expected for the correspondent solid polymers. The materials based on HDPE or on blends of HDPE and LDPE are more crystalline and have a higher thermal resistance than the foams based on LDPE or on the metallocene LDPE. Moreover, the foams based on EVA copolymers, because of the presence of the vinyl acetate monomer that reduces the regularity of the LDPE chains, have a lower degree of crystallinity and a lower melting point.

Finally, some of the foams under study (black foams) present a black carbon content in their initial formulation (between 3 and 12% in weight) (Table I). To obtain the crystallinity of these materials it is necessary to introduce a linear correction factor because of the different weight of polymer in these foams. This correction has not been

Table III. Microscopic and Thermal Characteristics of the Foams Under Study

Foams	$\Phi(\mu\text{m})$	$\xi(\mu\text{m})$	f_s	χ_c (%)	T_m (°C)
LD15W	313.5	1.4	0.22	40.6	105.9
LD18W	879.7	5.8	0.21	41.8	108.4
LD24W	311.9	1.9	0.16	43.8	108.6
LD29W	528.1	4.2	0.24	42.9	108.4
LD33W	424.4	3.6	0.28	43.9	105.8
LD33(1)W	396.9	2.5	0.36	41.6	108.6
LD50CNB	910.4	10.8	0.22	37.0	108.3
LD60 G	773.4	10.3	0.24	42.1	109.0
LD70B	528.1	6.0	0.35	40.8	106.6
HL34W	673.8	8.8	0.24	57.5	127.5
HL47W	764.6	9.8	0.39	57.2	127.8
HL79B	770.6	16.3	0.26	54.0	129.3
HL79W	892.9	17.7	0.42	58.5	128.1
HL79(2)W	1006.0	20.9	0.46	56.4	127.9
HL79(3)W	1075.7	27.9	0.46	55.0	128.5
HD30W	469.8	4.5	0.23	66.2	130.8
MP24W	162.7	0.9	0.23	42.3	108.1
MP45B1	460.1	2.6	0.37	43.3	108.6
VA25W	785.7	6.1	0.10	32.2	92.9
VA35W	469.8	6.1	0.14	32.5	92.6
VA65W	615.9	9.4	0.23	32.5	94.5
EV50O	406.0	4.3	0.42	24.2	78.5
EV50B	255.8	3.0	0.15	25.7	78.4

W = White, O = Orange, B = Black, Bl = Blue, G = Green. Φ is the cell size, ξ is the cell wall thickness, f_s is the fraction of solid in the struts, χ_c is the crystallinity, and T_m is the melting point.

made in the data presented in Table III, which explain the slightly lower value of the crystallinity of the black foams.

As we pointed out in the introduction an interesting conclusion can be inferred from the previous microscopic characterization. Zotefoams are

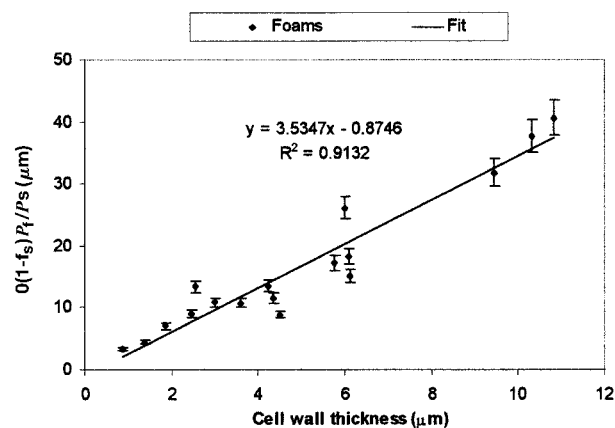


Figure 3. Experimental results and fit to the equation $\Phi(1-f_s)\rho_f/\rho_s = C\xi$ for the LD, HD, MP, VA, and EV foams.

excellent commercial materials for scientific studies because of some interesting features as the following: lack of residues of solid foaming agent on the final foam, almost isotropic cellular structure, same cell shape for the different densities, and very similar physical characteristics of the solid polymer that comprises the cell walls and of the solid sheet from which the foam was made. All these features are, of course, a consequence of the industrial high-pressure nitrogen gas solution process.

The previous microscopic structure is very different to that of polyolefin foams produced in a semi-continuous process based on a solid foaming agent.^{21,22} These foams exhibit residues of foaming agent in the cell walls, are anisotropic materials, and they present different cell shapes depending of the density. Therefore, these foams are more difficult to analyze from a scientific point of view.

Thermal Conductivity

The experimental thermal conductivity for all the foams under study, at room temperature (24 °C),

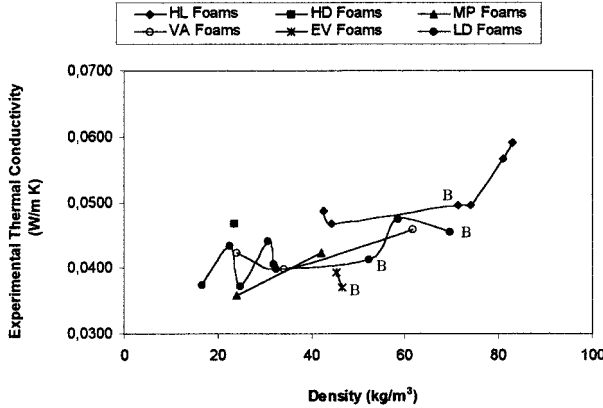


Figure 4. Experimental thermal conductivity as a function of the density for all the foams under study. B = Black foams.

as a function of the foam density is presented in Figure 4. The thermal conductivity does not show a clear trend with density. However, the shape of the curves, for each type of material, is similar to that of the cell size [Fig. 2(a)]. Therefore, it is clear that the cell size is an important parameter in the thermal conductivity of the foams. The smaller the cell size, the better insulation capabilities.

On the other hand, although the LD50CNB foam has the largest cells and thickest cell walls within the group of the LD foams (Table III), its thermal conductivity is not the largest (Table I). In order to clarify this behavior it is necessary to bear in mind another effect that is the reduction of the conductivity due to the presence of black carbon in the initial formulation of this foam. We will go over this point below.

DISCUSSION

The evaluation of the thermal conductivity of foams from the conductivity data of the two component phases (continuous solid phase and discontinuous gas phase) and the structure of the material is an important subject that has been approached by different authors.^{1–15} The thermal conductivity of these materials (λ) is due to four different mechanisms: conduction through the gas phase (λ_g), conduction along the cell walls and struts of the solid polymer (λ_s), convection within the cells (λ_c), and thermal radiation (λ_r). The total heat transfer can be predicted as the sum of the heat transfer by the four mechanisms considered

separately. It is widely accepted that convection plays a minor role in heat transfer in closed cell materials provided the cells are less than 4 mm in diameter.²³ Therefore, in this work, the convective heat transfer is assumed to be negligible because of the reduced volume of the cells, which is lower than the limit set above.

In the next section, we have applied some of these models to estimate the contribution of each heat-transfer mechanism to the whole thermal conductivity.

Conduction Through the Solid and Gas Phases

The term connected to the conduction through the solid and gas phases can be computed by using the following equation:⁶

$$\lambda_g + \lambda_s = \lambda_{\text{gas}} V_{\text{gas}} + \left(\frac{2}{3} - \frac{f_s}{3} \right) \lambda_{\text{poly}} V_{\text{poly}} \quad (3)$$

where λ_{gas} is the thermal conductivity of the gas, which fills the cells, λ_{poly} is the thermal conductivity of the matrix polymer, V_{gas} is the volume fraction of gas and V_{poly} is the volume fraction of polymer. The first term in the preceding equation is the contribution of the gas, and depends on its own nature. In our case, the gas is air at atmospheric pressure, for which the conductivity at room temperature is $\lambda_{\text{air}} = 0.0263$ W/m K. The gas in the cells is air, because gases can diffuse in and out of LDPE foams on a time scale of weeks.^{24,25} The second term in eq 3 is associated with the contribution of the solid phase. From the DSC results, we concluded that the solid polymer in the cell walls of the foams had similar characteristics compared to a solid sheet produced from the same polymer. Therefore, it is reasonable to use the measured value of the thermal conductivity of those solid sheets to estimate (λ_{poly}) in the previous equation (Table II).

Moreover, black foams should present an additional contribution to the heat transfer through the solid phase. Nevertheless, as a first approximation we have calculated the conduction through the solid phase using the same value of the solid polymer conductivity as that used for the other foams based of the same polymer. This approximation, as the results have shown, is valid due to the low weight of the conduction through the solid phase for this kind of foam (see below).

Radiation

This term can be estimated by subtracting the conduction through the solid and gas from the

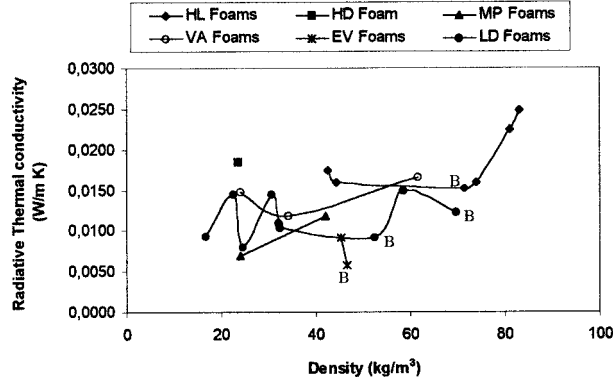


Figure 5. Radiative thermal conductivity as a function of the foam density for all the foams under study. B = Black foams.

experimental thermal conductivity (Fig. 5). The appearance of the radiation curves versus density are similar to that of the cell size versus density [Fig. 2(a)]; therefore, in the range of densities under study, the cell size plays an important role in the thermal radiation contribution of the foams. Consequently, it can be concluded that the dependence of the thermal conductivity with the cell size is mainly due to the dependence of the radiation term on this geometric parameter. Smaller isotropic cells result in a higher number of reflecting and absorbing surfaces, which reduces the radiation through the foam.

In order to be able to predict the radiation contribution, the following models were applied. Roseland,⁶ Glicksman,⁶ Boets and Hoogendoorn,¹¹ Williams and Aldao,⁹ Frank and Kingery.¹³

The best fit was obtained by using the Williams and Aldao model.⁹

$$\lambda_r = \frac{4\sigma T^3 L}{1 + \left(\frac{L}{\Phi}\right)\left(\frac{1}{T_N} - 1\right)} \quad (4)$$

where σ is the Stefan–Boltzman constant, T is the temperature, L is the foam thickness, Φ is the mean cell size and T_N is the net fraction of radiant energy sent forward by a solid membrane of thickness L_s (this quantity can be represented in our work by the mean cell wall thickness). It is given by:

$$T_N = \frac{(1 - r)}{(1 - rt)} \left\{ \frac{(1 - r)t}{(1 + rt)} + \frac{(1 - t)}{2} \right\} \quad (5)$$

where r is the fraction of incident energy reflected by each gas–solid interface. This quantity is related to the refractive index of the plastic ω by:

$$r = \left\{ \frac{\omega - 1}{\omega + 1} \right\}^2 \quad (6)$$

Table IV. Main Characteristics of the Foams Used To Check the Effect of the Thickness on the Thermal Conductivity

Foams	ρ_f (kg/m ³)	L (mm)	χ_c (%)	T_m (°C)	Φ (μm)	λ (W/m K)
LD15(0)W	16.7	11.2	40.6	105.9	313.5	0.0374
LD15(2)W	18.4	19.8	44.3	105.8	313.5	0.0382
LD15(3)W	18.0	30.0	44.8	105.8	313.5	0.0389
LD24(0)W	24.6	10.3	43.8	108.6	311.9	0.0372
LD24(1)W	24.3	16.3	45.9	108.8	328.5	0.0377
LD24(2)W	22.9	20.1	41.1	108.9	328.5	0.0375
LD24(3)W	23.5	30.1	43.1	108.9	328.5	0.0367
LD33(0)W	32.0	11.0	43.9	105.8	424.4	0.0407
LD33(1)W	31.4	15.1	42.2	108.9	376.8	0.0401
LD33(2)W	31.8	20.2	42.9	108.8	376.8	0.0415
LD33(3)W	31.5	29.8	42.4	108.8	376.8	0.0413
LD45(1)W	42.6	14.9	41.4	108.8	387.3	0.0427
LD45(2)W	41.9	20.8	44.2	108.8	387.3	0.0438
LD45(3)W	42.0	29.2	45.3	109.0	387.3	0.0422

ρ_f is the foam density, L is the thickness, χ_c is the crystallinity, T_m is the melting point, Φ is the cell size, and λ is the thermal conductivity.

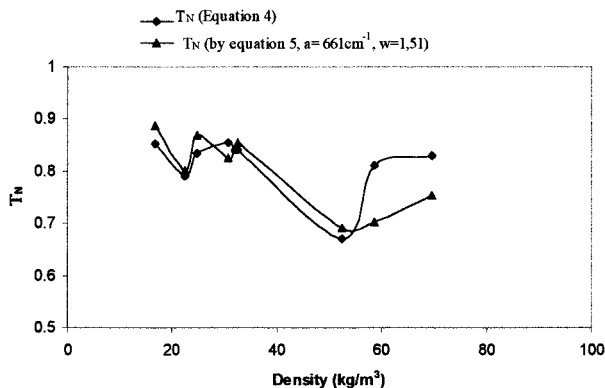


Figure 6. T_N values as a function of the density for the LD foams obtained by two different methods.

and the coefficient t is the fraction of energy transmitted through the solid membrane (thickness L_s), which is given by the Bouguer's law:

$$t = \exp(-aL_s) \quad (7)$$

where a is the absorption coefficient of the plastic.

Two important parameters, cell size (Φ) and foam thickness (L), are taken directly into account for the model. The predicted dependence on cell size is the same as that shown in our experimental results. Moreover, for the foams under study (cell sizes between 160 and 1000 μm), the model predicts an increase of the thermal radiation term for sample thicknesses lower than 10 mm, being the thermal radiation almost constant for foams of higher thicknesses. In order to check the previous prediction, the thermal conductivity of foams with the same characteristics (density, chemical composition, color, and cell size) and different thickness (between 10 and 30 mm) was measured. The results (Table IV) showed that the differences between the thermal conductivities are lower than 5% value, which is within the limit of uncertainty of the experimental results.

On the other hand, the dependence of the thermal radiation on other microscopic characteristics as, for example, the chemical composition, the matrix polymer morphology, and the cell wall thickness are taken into account by the model through the values of ω , a and L_s .

In order to check the validity of the Williams and Aldao model to describe our experimental results, we calculated T_N following two different ways. First, for each foam, we obtained T_N using eq 4 and the experimental results for the conductivity due to the thermal radiation (Fig. 5). Sec-

ond, using typical values for the refractive index, ω , and the absorption coefficient of the plastic, a , and the values of the cell wall thickness (Table III), we computed T_N by using eq 5.

The values of T_N as a function of the foam density for the LD foams, calculated from the two previous methods, are shown in Figure 6. The coincidence between the two curves is a confirmation of the validity of the model for describing the thermal radiation of the foams under study. The value for ω (1.51) is typical for LDPE²⁶ and a mean value for a (661 cm^{-1}) was used. This value is similar to that proposed by Glicksman.⁶

Each foam has its own T_N , which is a consequence of the dependency of this quantity on the cell wall thickness, chemical composition, and matrix polymer morphology. The numerical values of T_N for each material are summarized in Table V. However, and from a practical point of view, it is possible to predict accurately, the thermal radiation by using a mean value of T_N for each type of foam (see below). These mean values are also given in Table V.

On the other hand, an important result appears when the thermal conductivity of the white

Table V. Numerical Values of T_N for Each Foam Under Study and Mean Values for the Different Types

Foams	T_N (by eq 4)	Mean Values T_N
LD15W	0.852	
LD18W	0.790	
LD24W	0.834	
LD29W	0.855	
LD33W	0.840	0.831
LD33(1)W	0.840	
LD60G	0.810	
LD70B	0.830	
LD50CNB	0.670	0.67
HL34W	0.860	
HL47W	0.827	
HL79W	0.820	0.841
HL79(2)W	0.860	
HL79(3)W	0.840	
HL79B	0.816	0.816
HD30W	0.904	0.904
MP24W	0.890	
MP45W	0.844	0.867
VA25W	0.805	
VA35W	0.840	0.835
VA65W	0.860	
EV500	0.817	0.814
EV50B	0.810	

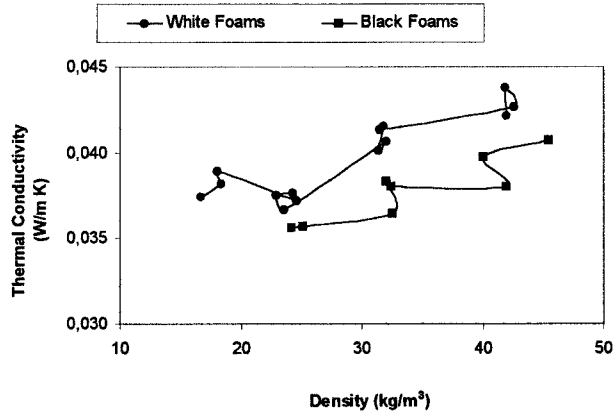


Figure 7. Experimental thermal conductivity for the white and black LD foams.

and black foams is compared (Fig. 7). The black foams have a lower thermal conductivity. These materials also have a higher extinction coefficient (in average 27 cm^{-1}), which results in a lower thermal radiation. This result can be also understood by using the Williams and Aldao model. Because of the black carbon content, the cell walls of the polymer have different refractive index and absorption coefficient, which results in different T_N values. While the LD white foams have, in average, a T_N value of 0.831 ± 0.008 , the black foams have an average value of 0.790 ± 0.007 .

From the previous discussion, there is one result we want to underline. By using the following equation:

$$\lambda = \lambda_{\text{gas}} V_{\text{gas}} + \left(\frac{2}{3} - \frac{f_s}{3} \right) \lambda_{\text{poly}} V_{\text{poly}} + \frac{4\sigma T^3 L}{1 + \left(\frac{L}{\Phi} \right) \left(\frac{1}{T_N} - 1 \right)} \quad (8)$$

in which all the quantities can be experimentally determined and/or estimated, the thermal conductivity of polyolefin foams produced from a high-pressure nitrogen gas solution process can be computed with a good precision. The error of the predicted value is approximately $\pm 2.6\%$.

A first application of the previous equation is the calculation of the relative weights of each of the heat flow mechanisms in the final conductivity (Fig. 8). It can be observed that the main contributions for these low-density foams based on polyolefins are the conduction through the gas and the thermal radiation. An improving of the thermal conductivity of these products could be reached by modifying the parameters that control these two heat-transfer mechanisms.

Moreover, by using eq 8, it is possible to separate the dependence of the thermal conductivity with different parameters, which it is usually very difficult in experimental studies. An example is presented in Figure 9. The thermal conductivity at $T = 24 \text{ }^\circ\text{C}$ of a low-density polyethylene foam (density 58.5 kg/m^3) has been computed by using eq 8 as a function of the cell size and for different values of f_s . The parameters used to

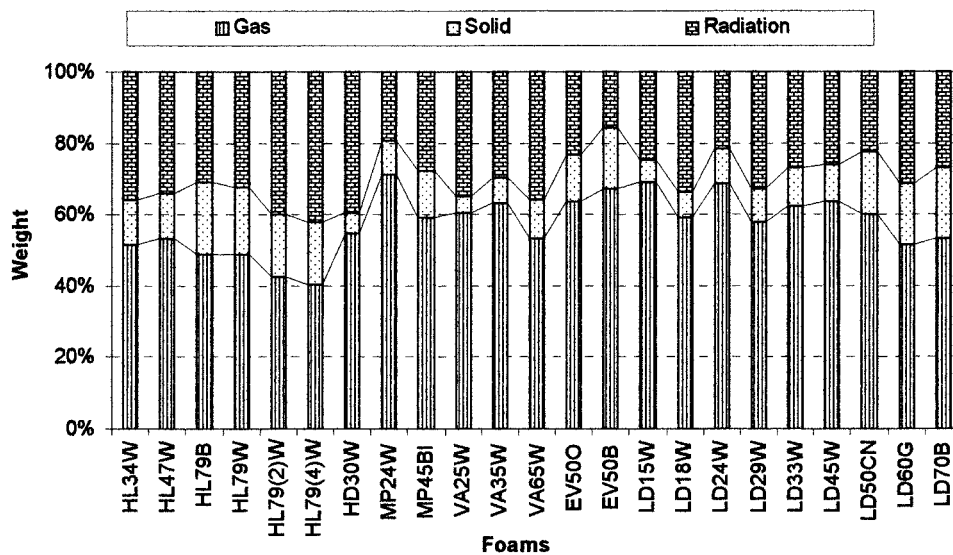


Figure 8. Weights of the analyzed heat flow mechanism in the whole thermal conductivity.

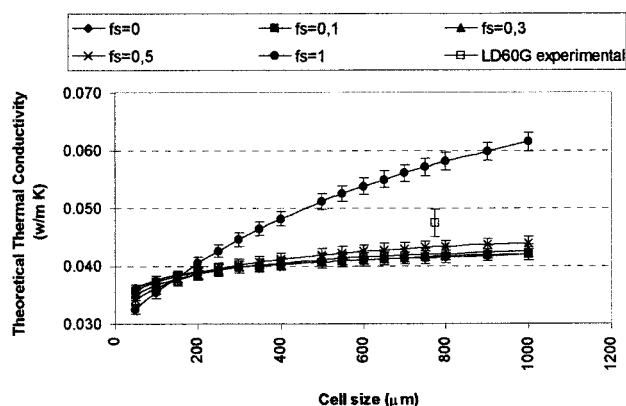


Figure 9. Theoretical thermal conductivity (LD60G foam) as a function of the cell size and for different values of the mass fraction in the struts (using eq 8).

calculate the thermal conductivity were $\lambda_{\text{poly}} = 0.214$ W/m K, $\lambda_{\text{gas}} = 0.0263$ W/m K, $V_{\text{gas}} = (1 - \rho_f/\rho_0) = 0.936$, $V_{\text{poly}} = (\rho_f/\rho_0) = 0.064$, $L = 10.2$ mm. The value of T_N was calculated by means of equations 5, 6, and 7. A refractive index $\omega = 1.51$ and an absorption coefficient $\alpha = 661$ cm^{-1} were used. The mean cell wall thickness ξ (L_s in eq 7) was calculated, for each cell size and mass fraction in the struts, using eq 2 with a C value of 3.53.

The predicted thermal conductivity is very close to experimental value (difference 7%). Moreover, the quantitative dependence of the thermal conductivity on cell size and mass fraction in the struts can be deduced from that plot (the effect of other important parameters is eliminated). As can be observed, a reduction in the mass fraction of the strut, for a given cell size and shape, results in a lower thermal conductivity. This can be explained by taking into account that a lower mass fraction in the struts is related to a higher mean cell wall thickness, which reduces the thermal radiation.

CONCLUSIONS

The thermal conductivity of a collection of closed cell polyolefin foams has been studied, in terms of the microscopic characteristics of the materials. An equation without adjustable parameters has been presented to compute the thermal conductivity of these materials. The experimental results showed that this equation predicts thermal conductivity values with a good precision (differences between the experimental and the calcu-

lated values lower than 7%). The effect of the density, gas and solid conductivity, fraction of mass in the struts, cell size, thickness, chemical composition, and matrix polymer morphology are taken into account in the previous equation. Finally, three interesting results have been pointed out:

1. Black foams with a low carbon content have lower thermal conductivities due to the reduction of the thermal radiation term;
2. The main contribution to the whole thermal conductivity for these low-density foams based on polyolefins is the conduction through the gas;
3. The thermal radiation and the dependence of the thermal conductivity on cell size has been quantified.

Financial assistance (Ovidio A. Almanza) from COLCIENCIAS (Colombia) is gratefully acknowledged. The authors thank Zotefoams Plc. for supplying the foams.

NOMENCLATURE

ρ_f	Foam density
ρ_0	Polymer base density
L	Foam thickness
k_{exp}	Extinction coefficient
λ	Thermal conductivity
θ_{carbon}	Black carbon content
χ_c	Crystallinity
T_m	Melting point
Φ	Mean cell diameter
ξ	Mean cell wall thickness
f_s	Mass fraction in the struts
λ_s	Thermal conductivity due to the conduction through the solid phase
λ_g	Thermal conductivity due to the conduction through the gas phase
λ_r	Thermal conductivity due to the radiation
λ_c	Thermal conductivity due to the convection
λ_{poly}	Thermal conductivity of the polymer
λ_{gas}	Thermal conductivity of the gas
V_{poly}	Volume fraction of solid
V_{gas}	Volume fraction of gas
σ	Stefan–Boltzman constant
T	Temperature

T_N	Net fraction of radiant energy sent forward by a solid membrane
r	Fraction of the incident energy reflected by each solid-gas interface
t	Fraction of energy transmitted through a solid membrane
ω	Refractive index of the plastic
a	Absorption coefficient of the plastic
L_s	Thickness of a solid membrane
LDPE	Low-density polyethylene
HDPE	High-density polyethylene
EVA	Ethylene vinyl acetate copolymer

REFERENCES AND NOTES

1. Russel, R. H. *J Am Ceram Soc* 1935, 18(1), 1–5.
2. Leach, A. G. *J Phys D: Appl Phys* 1993, 26, 733–739.
3. Bedeaux, D.; Kapral, R. *J Chem Phys* 1983, 79, 1783.
4. Collishaw, P. G.; Evans, J. R. G. *J Mater Sci* 1983, 29, 486–498.
5. Kuhn, J.; Ebert, H. P.; Arduini-Schuster, M. C.; Büttner, D.; Fricke, J. *Int J Heat Mass Transfer* 1992, 35(7), 1795–1801.
6. Glicksman, L. R. In *Low Density Cellular Plastics: Physical Basis of Behaviour*; Hilyard, N. C.; Cunningham, A., Eds.; Chapman & Hall: London, 1994.
7. Cunningham, A. *Proc Int Cent Heat Mass Trans* 1987, 24, 32.
8. Schuetz, M. A.; Glicksman, L. R. *J Cell Plast* 1984, 20(2), 114–121.
9. Williams, R. J. J.; Aldao, C. M. *Polym Eng Sci* 1983, 23, 32.
10. Ball, G. W.; Hurd, R.; Walker, M. G. *J Cell Plast* 1970, 66(2), 66–78.
11. Boetes, R.; Hoogendoorn, C. J. *Proc Int Cent Heat Mass Trans* 1987, 24, 14.
12. Loeb, A. L. *J Am Ceram Soc* 1954, 37, 96.
13. Francl, J.; Kingery, W. D. *J Am Ceram Soc* 1954, 37, 99.
14. Batty, W. J.; Probert, S. D.; O'Callaghan, P. W. *Appl Energy* 1984, 18, 117.
15. Almanza, O.; Rodríguez-Pérez, M. A.; de Saja, J. A. *Cell Polym, Cellular Polymers*, 18(6), 385, 1999.
16. Sims, G. L. A.; Kunniteekoll, C. *Cell Polym* 1994, 13, 137.
17. ASTM D3576, *Annual Book of ASTM Standards*, 1994; Vol. 8.02.
18. Wunderlich, B. In *Macromolecular Physics*; Academic Press: New York, 1973–1976; Vol 2.
19. Rodríguez-Pérez, M. A.; Alonso, O.; Souto, J.; de Saja, J. A. *Polym Test* 1997, 16, 287.
20. Mills, N. J.; Gilchrist, A. *J Cell Plast* 1997, 33, 1264.
21. Rodríguez-Pérez, M. A.; Alonso, O.; Duijsens, A.; de Saja, J. A. *J Polym Sci Polym Phys Ed* 1998, 36, 2587–2596.
22. Rodríguez-Pérez, M. A.; Duijsens, A.; de Saja, J. A. *J Appl Polym Sci* 1998, 68, 1237–1244.
23. *Heat Transfer*; Holman, J. P., Ed.; McGraw-Hill: New York, 1981.
24. Mills, N. J.; Gilchrist, A. *Cell Polym* 1997, 16, 87.
25. Mills, N. J. In *Foams and Emulsions*, NATO ASI Series; Sadoc, J. F.; Rivier, N., Eds.; 1999.
26. *Handbook of Plastics Testing Technology*; Vishu, S., Ed.; Wiley: New York, 1984.